POLITECNICO DI TORINO
Repository ISTITUZIONALE

Metallic mirrors for plasma diagnosis in current and future reactors: tests for ITER and DEMO

(Article begins on next page)

21 December 2024

Metallic mirrors for plasma diagnosis in current and future reactors: Tests for ITER and DEMO

M. Rubel[a*], A. Garcia-Carrasco[a], Soonwoo Moon[a], P. Petersson[a], A. Hallén[a], A. Krawczynska[b], E. Fortuna-Zaleśna[b], M. Gilbert[c], T. Płociński[b], A. Widdowson[c] and JET Contributors**

EUROfusion Consortium, JET, Culham Science Centre, OX14 3DB, Abingdon, UK

[a]*Royal Institute of Technology (KTH), SE-10044 Stockholm, Sweden*

[b]*Department of Materials Science, Warsaw University of Technology, 02-502 Warsaw, Poland*

[c]*Culham Centre for Fusion Energy, Culham Science Centre, Abingdon, OX14 3DB, UK*

*Corresponding author: tel.: +46 8 790 6093, e-mail: Marek.Rubel@ee.kth.se

**See the author list of "Overview of the JET results in support to ITER", X. Litaudon et al., in press Nuclear Fusion Special issue: 26th Fusion Energy Conference (Kyoto, Japan, 2016)

Abstract

Optical spectroscopy and imaging diagnostics in next-step fusion devices will rely on metallic mirrors. The performance of mirrors is studied in present-day tokamaks and in laboratory systems. This work deals with comprehensive tests of mirrors: (a) exposed in JET with the ITER-Like Wall (JET-ILW); (b) irradiated by hydrogen, helium and heavy ions to simulate transmutation effects and damage which may be induced by neutrons under reactor conditions. The emphasis has been on surface modification: deposited layers on JET mirrors from the divertor and on near-surface damage in ion-irradiated targets. Analyses performed with ion beams, microscopy and spectro-photometry techniques have revealed: (i) the formation of multiple co-deposited layers; (ii) flaking-off the layers already in the tokamak, despite small thickness (130-200 nm) of the granular deposits; (iii) deposition of dust particles (200 nm- 5 μm, 300-400 mm^{-2}), especially tungsten and nickel; (iv) the stepwise irradiation up to 30 dpa by heavy ions (Mo, Zr or Nb) caused only small changes in the optical performance, in some cases even improving even reflectivity due to the removal of surface oxide layer; (v) significant reflectivity degradation related to bubble formation caused by the irradiation with He and H ions.

Keywords: plasma, diagnostic mirrors, beryllium, irradiation, JET-ILW

PACS: 52.40.Hf

1. Introduction

Plasma operation either in low- or high-temperature systems requires reliable diagnosis of parameters. It is realized mainly by transmitting signals via optical means based on windows and mirrors [1]. In a thermonuclear reactor intense X-ray and gamma radiation would degrade transmissivity of windows. Therefore, metallic mirrors (so-called first mirrors) will have to be the plasma-facing components of optical arrangements for guiding light to various cameras and spectrometers. The transmission of all signals is to rely on such mirrors and simultaneously a proper neutron shielding must be maintained. To fulfil these conditions mirrors will be placed in labyrinthine path in the shielding block.

Processes of plasma-wall interactions (PWI) may strongly modify surfaces especially of first mirrors and, as a result, lead to the degradation of their optical performance, i.e. decrease of reflectivity. In current controlled fusion devices with magnetic confinement effects of material migration, i.e. erosion and deposition, are decisive for the change of specular reflectivity. In a reactor fuelled with a deuterium-tritium mixture these processes will occur in parallel to neutron-induced effects such as transmutation accompanied by the formation of gaseous species (H isotopes and He) and in the presence of helium produced in the D+T reaction.

To recognise the extent of different factors which may or will influence the performance of mirrors, there is abroad programme aiming at the assessment of property changes under: (i) exposure to a fusion environment in tokamaks [2-12], (ii) irradiation by light species (H, He) and heavy ions to simulate effects on neutron impact on the optically active layer of mirror surfaces [13]. The degradation of optical properties of mirrors has been clearly demonstrated [3-12]. Therefore, the research programme comprises both the development of means for mirror protection [14,15] and cleaning [16-20]. Until now the best results are expected to be provided by a complex structure of diagnostic ducts [14], while no cleaning (or recovery) techniques have been proven successful and/or practical. Laser-induced cleaning which was tested on mirrors from JET with carbon walls (JET-C) resulted either in a very serious surface damage (micro-cracks and melting) by deposited energy [16] or only partial layer removal [17]. Plasma-induced cleaning resulted in the layer removal but it was associated with a significant increase of diffuse reflectivity, i.e. degradation of specular component [19]. Layer removal was achieved from mirrors coated by films prepared under laboratory conditions, however such films do not have properties of co-deposits formed in tokamaks. The only case of reflectivity recovery for mirrors from the JET tokamak was

achieved by polishing [21], but this approach is impractical because the mirror treatment was carried out ex-situ. In such case, a periodic replacement of mirrors would be a better solution.

In ITER (International Thermonuclear Experimental Reactor) there will be several tens of first mirrors for plasma diagnosis [22]. This situation leads to a conclusion that at least three technically demanding engineering pathways should be pursued: (i) careful design of diagnostic channels still not compromising the quality of the received signal: (ii) options for mirror replacement and (iii) in-situ efficient cleaning. The latter one also calls for means to assess the reflectivity recovery over the entire mirror surface. For the development and testing of cleaning methods the most important is the knowledge of the surface state. Results on mirror testing from JET-C and JET-ILW have provided a consistent picture: relatively small changes in the reflectivity for mirrors on the main chamber wall and very significant reflectivity loss for all mirrors in the divertor [3-7]. From the cleaning point the knowledge of the worst cases is the most important, i.e. the state of the mirror surfaces from the divertor.

The objective of this contribution is to provide an account, as detailed as possible, of surface changes of molybdenum mirrors exposed at the JET tokamak with the ITER-Like Wall (JET-ILW), i.e. with beryllium and tungsten plasma-facing components (PFC). The second point is the degradation of optical properties expected under neutron impact causing changes in structure (damage) and composition (transmutation). The work is directed towards studies of phenomena which with occur next-step fusion devices.

2. Experimental

2.1. Mirrors

The study was carried out with two types of polycrystalline molybdenum mirrors: (i) exposed in the divertor of JET tokamak during the second campaign with the ITER-Like Wall (ILW-2) and (ii) irradiated both by heavy (Mo, Zr, Nb) and light (H, He) ions. Test specimens at JET were placed in cassettes or pan-pine shape and installed in three locations in the divertor: in the base under the bulk tungsten tile (Tile 5) and in the shadowed regions of the inner and outer leg; details of cassette construction and installation can be found in [2,6]. A figure of merit for mirrors in the channel of the cassette is the solid angle for particle bombardment. It was around 6×10^{-3} sr for the outer divertor mirror located 3.0 cm deep in the channel and 8×10^{-3} sr for the one from the divertor base placed 2.8 cm deep from the channel mouth. The

specimen in the inner was installed directly at the entrance to the channel. The exposure time was 19.5 h of plasma operation including 6 h of limiter discharges and 13,5 h of X-point plasma. The total energy input during the campaign was 201 GJ. In terms of time this correspond to 122 ITER discharges (400 s, Q = 10), but only to four ITER pulses scaled by energy input and about one ITER discharge in terms of divertor fluence [24].

Neutrons will interact with the surface and the bulk of components. For mirror it is the surface region which is important. Therefore, the irradiation programme has been based on SRIM [23] predictive modelling to define the irradiation conditions. This had to match the optically active layer in molybdenum mirrors, which extends to around 15-20 nm, as determined in [13]. To simulate neutron-induced effects the irradiation was done with 30 keV $^{98}Mo^+$, $^{93}Zr^+$, $^{90}Nb^+$, 2 keV He^+ and 4 keV H_2^+ ions. The irradiation with either zirconium or niobium was done, because both elements are formed as transmutation products in neutron-irradiated molybdenum. The damage of Mo in a reactor is foreseen to be 7 dpa and this would be accompanied by the presence of 45 appm of H, 479 appm of He [25,26]. The amount of Zr and Nb would be $1x10^{14}$ cm^{-2} and $1x10^{13}$ cm^{-2} in the surface layer of 15 nm. Graphs in Fig. 1 show the implantation and displacement rage of the implanted heavy ions. The irradiations were performed at the Ion Technology Centre (ITC) of the Ångström Laboratory at the Uppsala University, Sweden. A 350 kV Danfysik 1090 implanter with a beam current of up to 1 mA was used.

2.2. Analysis

Before and after exposure, mirrors underwent a detailed surface analysis using optical methods, ion beam and microscopy techniques. For JET mirrors the total and diffuse reflectivity was measured in the range 350–1700 nm using a photo-spectrometer (GetSpec) system complying with work procedures on materials retrieved from JET, i.e. contaminated with beryllium and tritium [27]. Optical performance of ion-irradiated mirrors was determined in the wavelength range from 300 nm to 2400 nm with a dual-beam spectrophotometer Lambda 950, Perkin Elmer.

Ion beam analyses (IBA) were done at the 5 MeV Tandem Accelerator Laboratory of Uppsala University. Light species implanted in mirrors were measured by means of time-of-flight heavy ion elastic recoil detection analysis (ToF HIERDA) using a 12 MeV Si^{3+} beam, The probed depth and the depth resolution were 120 nm and 8 nm, respectively. In studies of test mirrors from JET-ILW a 36 MeV iodine ($^{127}I^{8+}$) beam was applied in ToF HIERDA,

while a 2.5 MeV ^{3}He$^+$ beam was used for nuclear reaction analysis (NRA). Several microscopy methods were used at the Warsaw University of Technology (Poland) to examine mirror morphology: scanning electron microscopy (SEM, Hitachi SU-8000 FE-SEM) combined with energy-dispersive X-ray spectroscopy using silicon drift detector (EDS, Thermo Scientific Ultra Dry) enabling beryllium detection. Focused ion beam system (FIB/SEM, Hitachi NB5000) was used to prepare lamellae-type cross-sections of co-deposits on mirrors from JET and the the ion-irradiated region in the implanted mirrors. They were studied with the scanning transmission electron microscopy (STEM, Hitachi HD27009 operated at the accelerating voltage of 200 kV and a JEOL 1200 transmission electron microscope (TEM) operating at 120 kV.

3. Results

3.1. *Mirrors from the JET Divertor*

Plots in Figure show total reflectivity of the not exposed reference mirrors and for two mirrors placed in a remote region of the divertor: in the base under Tile 5 (Mirror 126) and in the outer leg (Mirror 121). With respect to the initial values, the loss of reflectivity in the outer divertor is at least by a factor of two over the entire spectral range because of the deposited layers. Characteristics for both mirrors are not of the same shape what is at least partly related to the layer thickness. Depth profiles measured by means of ToF HIERDA are presented in Figure 3(a) and (b). For the layer of 150-200 nm thick the loss is large and uniform. For a thin film (50 nm) on the other mirror the loss has a not uniform "wavy" structure.

An image in Fig. 4 (a) shows a general overview of the mirror surface from the outer divertor. One perceives a significant number of small particles and there are also spots where the deposit peeled-off; the latter is marked with arrow. As inferred from this and other survey SEM images the areal density of small dust particles is around 300-400 mm^{-2}, i.e. on the same level as observed on dust monitors installed above the outer and inner divertor [28]. In Fig. 4(b)-(d) there are several types of particles found on the mirror surface: nickel and iron-nickel spherical droplets and ball-like tungsten sphere of the kind shown also in [28,29]. The origin of such "balls" has been associated with a coagulation of W flakes from the tungsten coatings on the carbon fibre composite divertor tiles. From the image in Fig. 4(d) one infers two features: (i) the "skin" is composed of fragments of at least two layers (place is encircled) and (ii) a single layer contains at least 700-1000 flakes which are from 200 nm to 400 nm in linear dimensions. With the thickness of around 100 nm the volume of single flakes is

approximately $1\text{-}2\text{x}10^{-14}$ cm^3 with less than $1\text{x}10^9$ W atoms. This at least double layer skin suggests a gradual growth of such spherical particles. One layer serves as a skeleton or scaffolding a second one. The coagulation of so tiny fragments yields a question whether the formation of such spheres is limited to machines with W coatings or would it also occur in a machine with bulk metal PFC is tungsten-rich deposits flake-off.

A striking feature is that in most cases, e.g. Fig. 4(c) and (b) their surfaces are clean. As determined with beryllium-sensitive EDS, they are not embedded or covered by a deposit but they reside on the surface. Only a particle shown in Fig. 4(b) is coated. This allows for a tentative suggestion that most of them were deposited on the mirror in the final stages of the ILW-2 campaign, when tie rods of Tile 6 were damaged and experiments aiming at the generation of run-away electrons were carried out. An important point is that particles they stick well to surfaces.

The density of particles (300-400 mm^{-2}) detected in different regions of the divertor would correspond to $7\text{-}10\text{x}10^9$ particles on the entire divertor surface of 25 m^2. This number is huge, but the mass of single particles is estimated to be less than 1 ng thus being in total of the order of a gram in the divertor

Details of the granular structure of the deposit are in Figures 5(a) and (b). One perceives a spot (3x3 μm) where a deposit was detached and flaked-off. This must happen already in a tokamak because a built up of another layer takes place. Taking into account that the deposit thickness, as determined by HIERDA and also directly measured on FIB-made cross-section, is below 200 nm one comes to a conclusion that even very fine layers may flake. In other words there is no way to determine a critical layer thickness when co-deposits detach. A complex structure of a 700 nm deposit on a mirror from the inner divertor is shown in Z-contrast images of TEM in Fig. 6(a) and (b).

3.2.   Ion-irradiated molybdenum mirrors

Three sets of plots in Figure 7(a)-(c) show a sequence of reflectivity changes after the irradiation with 30 keV niobium, zirconium and 2 keV helium ions. In all cases the reflectivity of the initial not irradiated mirror is plotted for reference. One perceives that the implantation of either ^{93}Zr$^+$ or ^{90}Nb$^+$ to the dose corresponding to the damage of 10 dpa does not change reflectivity in the near ultraviolet and visible range. There is only a certain decrease, around 5 %, in the reflection of the infrared light at the wavelength above 1000 nm. The same was observed under ^{98}Mo$^+$ up to 30 dpa [13]. Distinctly stronger effects are caused by helium, because the gradual decrease of optical performance with the ion dose is in the

entire spectral range. Also for the mirror irradiated first with $^{90}Nb^+$ and then with $^4He^+$ the changes are caused by helium. The authors realise that the implanted dose of He is greater than the amount of atoms which would be produced by the transmutation, but it is also understood that under reactor conditions there will be a strong source of helium from the D-T fusion. Still stronger impact on the degradation of optical performance has been caused by hydrogen ions.

The change of reflectivity must be connected with the state of the optically active layer. The irradiated mirrors were examined with SEM and then lamellae-type cross-sections were manufactured by FIB for transmission microscopy (TEM and STEM) studies. An overview and very details of the structure in the near surface region is in Figure 8(a) and (b) for the Nb irradiated target, while images (c) and (d) have been recorded for a specimen implanted also with helium. These pictures were obtained in the Z-number contrast mode which is best suited for the detection of possible bubbles or blisters. No such structures are perceived in the Nb-irradiated material, while helium impact causes the formation of large blisters (20 nm) and a zone with small bubbles. That zone extends to the depth of 40 nm being in perfect agreement with the range of helium containing-zone measured by depth profiling by ToF heavy ion elastic recoil detection analysis. SEM and STEM documentation for surface and near surface region of the target irradiated with Nb and then with He and H ions is in Figure 9(a) and (b), respectively. The entire surface is uniformly covered by blisters 10 nm to 50 nm in diameter. Their density is 400-500 per 1 μm^2 of the sample area. The examination on the cross-section clearly confirms the density and the size of regular spherical. The examination at a greater magnification has revealed the existence of two types of bubbles: those big very close to the surface and smaller forms (2-5 nm) up to the depth 35-40 nm. One may assume that this is a mixture of bubbles produced both by He and H implantation.

4. Concluding remarks

The major contribution of this work to the progress in the study of first mirrors for fusion plasma diagnosis is the very detailed examination of surface changes caused by plasma-wall interactions. The changes of optical performance have been correlated with the surface morphology. The aim of research could be achieved and this has been possible due to a combination of relevant materials for studies and the application of a wide range of very sensitive high-resolution techniques for surface and sub-surface studies. To our knowledge these are the first-ever so detailed data on the composition of mirrors exposed in a tokamak..

In addition to co-deposits there are large quantities of small (200 nm – 8 μm) particles representing most of earlier identified [28-30] categories of dust. The presence of such particles certainly adds to the surface roughness and further degradation of optical signals. The results presented above, not uniform deposition, peeling-off layers and dust, add to the list of challenges in the development of in-situ methods for mirror cleaning.

Plasma diagnosticians in a reactor-class machine will be confronted with impact of radiation damage and related effects on the diagnostic components. The work carried out with ions is considered only as a first step in the assessment of optical mirror performance under nuclear environment. Until now, materials irradiated by heavy ions (e.g. damage of tungsten by W ions [23-25]) have been used mainly to assess the impact of damage on fuel retention. Data presented in [13] and in this paper indicate a broad range of factors having crucial consequence for mirrors. In summary, the results obtained by a set of optical, ion beam analysis and microscopy techniques perfectly confirm the right choice of the irradiation conditions with various species. They also explain the change of optical performance caused by various species that may and/or will affect surfaces of first mirrors in a fusion reactor.

References

[1] Donné A JH, Costey AE, 2004 *IEEE Trans. Plasma Sci.* **32** 177

[2] Rubel M *et al* 2006 *Rev. Sci. Instrum.* **77** 063501

[3] Rubel M *et al* 2009 *J. Nucl. Mater.* **390-391** 1066.

[4] Rubel M *et al* 2011 *Phys. Scr.* **T145** 014070

[5] Rubel M *et al* 2010 *Nucl. Instrum. Meth.* **A623** 818

[6] Ivanova D *et al* 2014 Phys. Scr. **T159** 012011.

[7] Garcia-Carrasco A *et al* 2017 *Nucl. Mater. Ener.* http://dx.doi.org/10.1016/j.nme.2016.12.032

[8] Wienhold P *et al* 2005 *J. Nucl. Mater.* **337** 1116.

[9] Litnovsky A *et al* 2007 *J. Nucl. Mater.* **363-365** 1395.

[10] Lipa M *et al* 2006 *Fusion Eng. Des.* **81** 221.

[11] Zhou Y *et al* 2006 *Fusion Eng. Des.* **81** 2823.

[12] Ono K *et al* 2009 *Phys. Scr.* **T138** 014065.

[13] Garcia-Carrasco A *et al* 2016 *Nucl. Instr. Meth.* **B382** 91

[14] Vizvary Z *et al* 2017 *Fusion Eng. Des.*http://dx.doi.org/10.1016/j.fusengdes.2016.12.016

[15] Litnovsky A *et al* 2015 *Nucl. Fusion* **55** 093015

[16] Leontyev A *et al* 2011 *Fusion Eng. Des.* **86** 1726

[17] Wisse M *et al* 2014 *Fusion Eng. Des.* **89** 122

[18] Skinner CH *et al* 2005 *J. Nucl. Mater.* **337–339** 129.

[19] Moser L *et al* 2016 *Phys. Scr.* **T167** 014069

[20] Litnovsky *et al* 2011 *Fusion Eng. Des.* **86** 1780

[21] Ivanova D *et al* 2013 *J. Nucl. Mater.* **438** S1241

[22] Costley A *et al* 2005 *Fusion Eng. Des.* **74** 109

[23] Ziegler JF *et al* 1996 *The stopping and range of ions in solids.* 2nd ed. New York, Pergamon

[24] Pitts RA *et al* 2005 *Plasma Phys. Control. Fusion* **47** B300

[25] Gilbert MR and Sublet J-Ch, 2015 *Handbook of activation, transmutation, and radiation damage properties of the elements simulated using FISPACT-II & TENDL-2014; Magnetic Fusion Plants*, Tech. Rep. CCFE-R(15)26, CCFE

[26] Gilbert MR and Sublet J-Ch, 2015 *PKA distributions of the elements simulated using TENDL-2014*, Tech. Rep. CCFE-R(15)26-supplement, CCFE

[27] Widdowson A *et al* 2016 Phys. Scr. **T167** 014057

[28] Fortuna E *et al* 2017 *These proceedings*

[29] Baron-Wiechec A *et al* 2015 *Nucl. Fusion* **55** 113033

[30] Fortuna E *et al* 2017 *Nucl. Mater. Energy* http://dx.doi.org/10.1016/j.nme.2016.11.027

[31] Ogorodnikowa O *et al* 2011 *J. Nucl. Mater.* **415** S661

[32] Grzonka J *et al* 2014 *Nucl. Instr. Meth.* **B 340** 27.

[33] Ogorodnikowa O *et al* 2014 *J. Nucl. Mater.* **451** 379.

Figure captions

Figure 1.
SRIM simulations of: (a) implantation depth profile in a Mo mirror under Zr and Nb irradiation; (b) damage depth profile of a Mo mirror under irradiation by Zr and Nb. The optically active layer is marked in blue.

Figure 2.
Total reflectivity of mirrors exposed during the second campaign of JET-ILW in the base and in the outer divertor. The initial reflectivity is shown.

Figure 3.
Depth profiles obtained by ToF-HIERDA for elements in co-deposits on mirrors during the second campaign of JET-ILW in (a) the outer divertor and (b) in the base.

Figure 4.
Micrographs showing general features and details of surfaces of mirrors exposed during the second campaign of JET-ILW in the base and in the outer divertor: (a) survey image with dust particles and peeled-off deposits; (b) spherical Fe+Ni droplet; (c) spherical Ni droplet; (d) spherical tungsten ball-like particle.

Figure 5.
Micrographs of a co-deposit on the mirror from the outer divertor: (a) area with peeled-off layer; (b) details of the deposit structure.

Figure 6.
Transmission electron microscopy of the co-deposit from the inner divertor mirror: (a) overview image and (b) details of the structure.

Figure 7.
Variation of reflectivity of molybdenum mirrors under: (a) irradiation with $^{90}Nb^+$ corresponding to 10 dpa; (b) He^+ irradiation with two different fluency levels; (c) Irradiation with $^{90}Nb^+$ and $^4He^+$ ions.
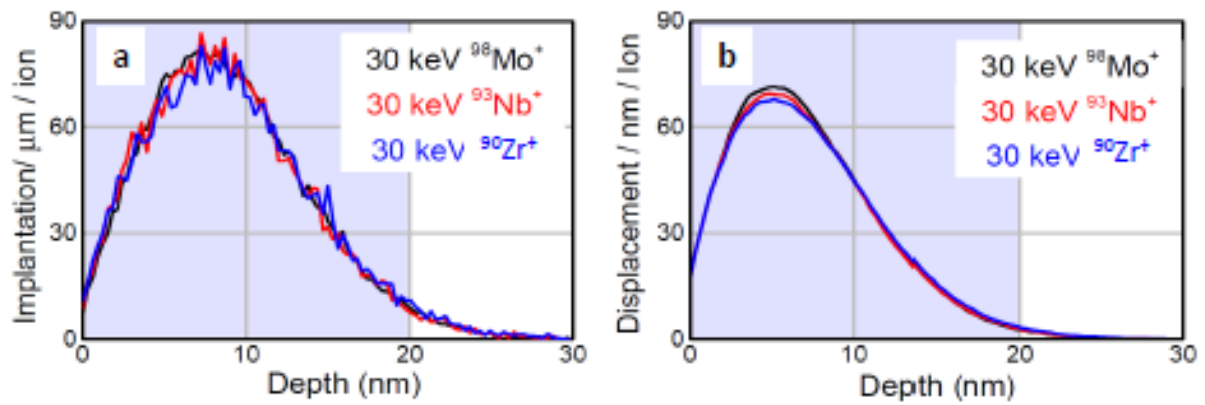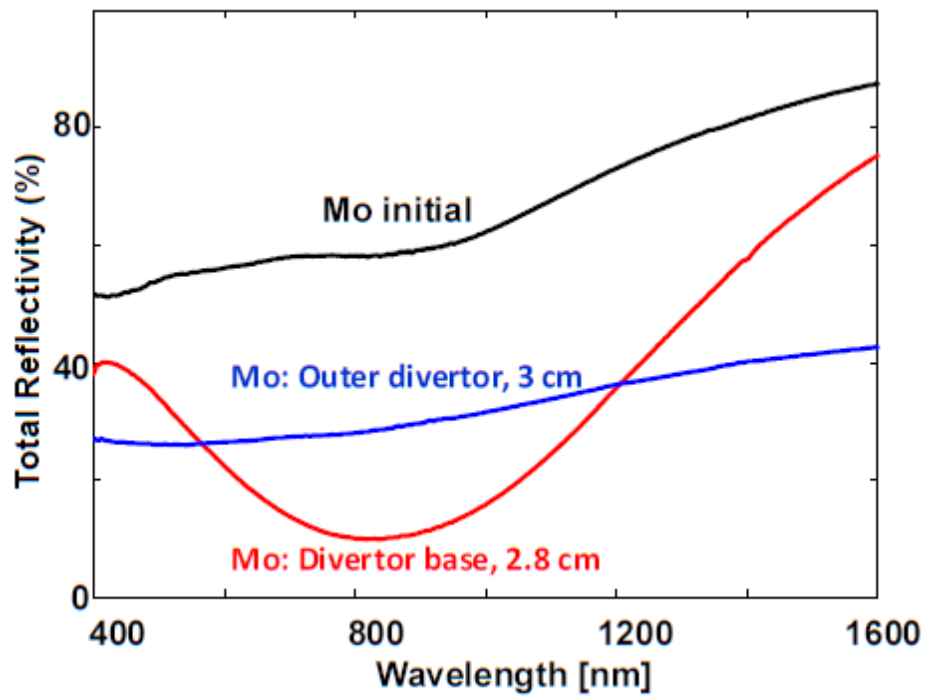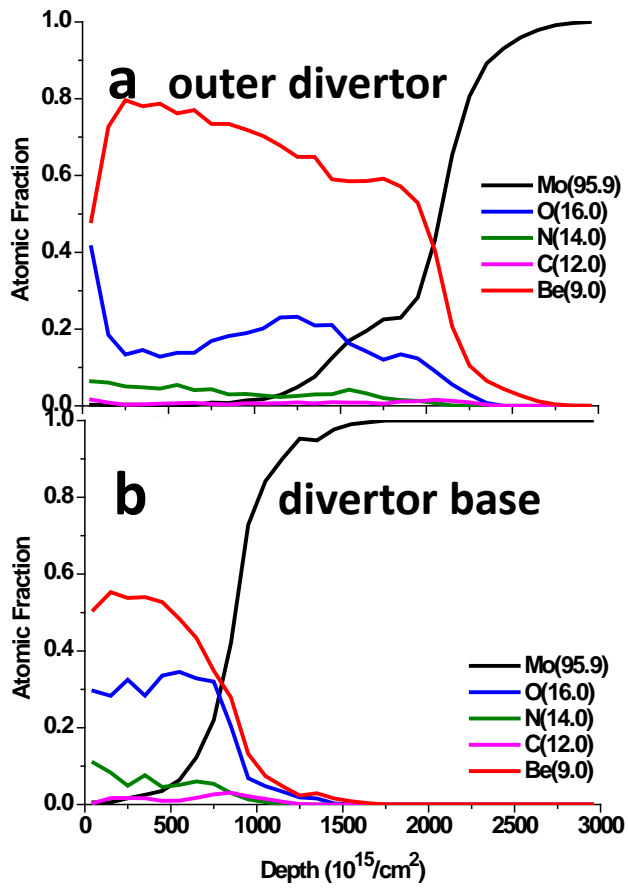
Figure 8.

Results of scanning transmission electron microscopy of molybdenum mirrors irradiated with: (a) and (b) with $^{90}Nb^+$ ions; (c) and (d) both with $^{90}Nb^+$ and with $^4He^+$ ions.

Figure 9.

Micrographs of the (a) surface and (b) sub-surface region of the Mo mirror irradiated first with $^{90}Nb^+$ and then with helium and hydrogen ions.

Figure 1

SRIM simulations of: a) implantation depth profile in a Mo mirror under Zr and Nb irradiation; b) damage depth profile of a Mo mirror under irradiation by Zr and Nb. The optically active layer is marked in blue.

Figure 2.

Total reflectivity of mirrors exposed during the second campaign of JET-ILW in the base and in the outer divertor. The initial reflectivity is shown.
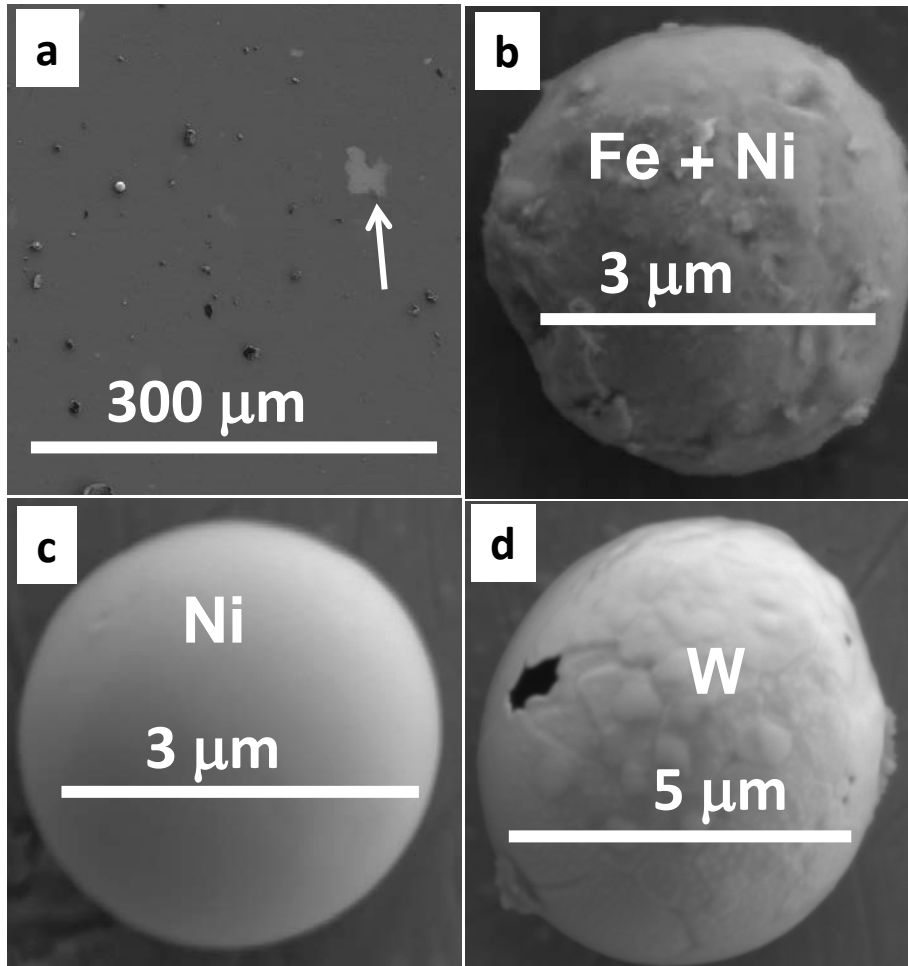
Figure 3.

Depth profiles obtained by ToF-HIERDA for elements in co-deposits on mirrors during the second campaign of JET-ILW in (a) the outer divertor and (b) in the base.
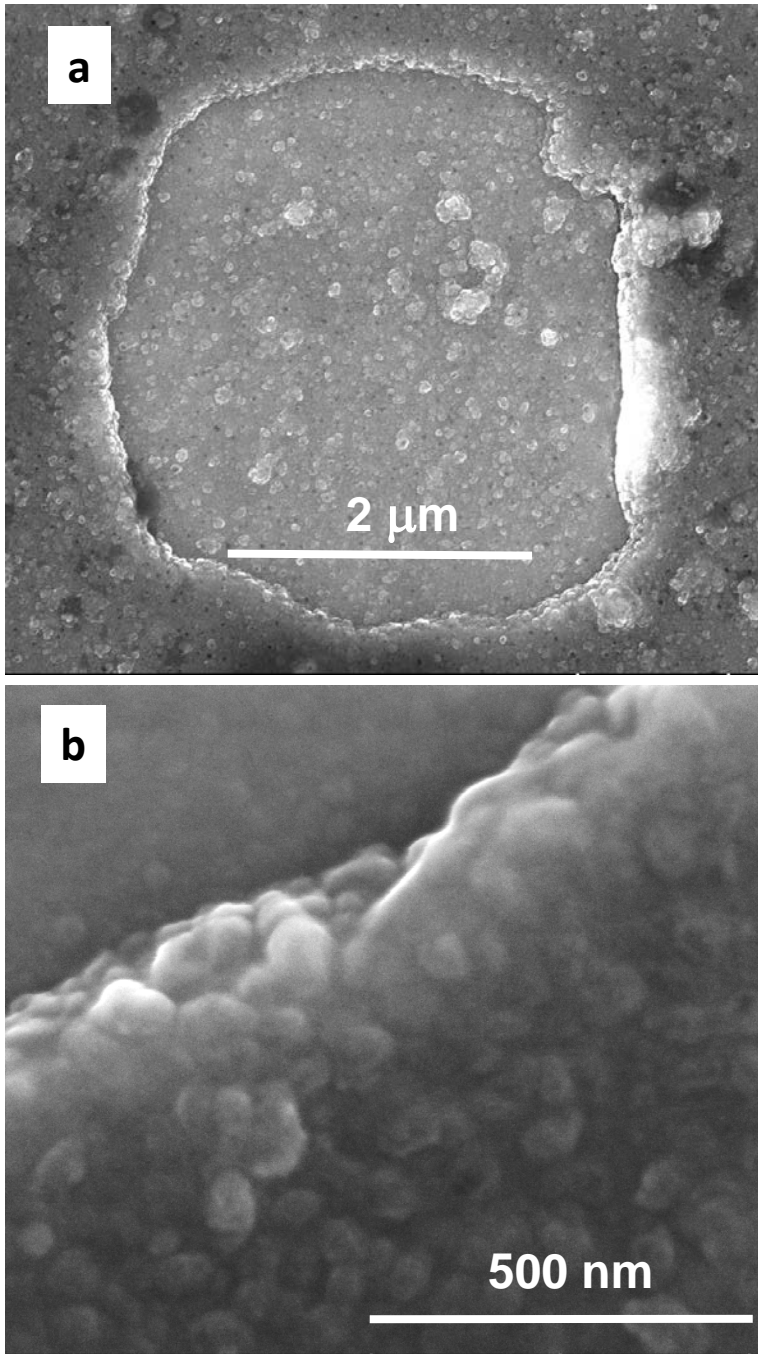
Figure 4

Micrographs showing general features and details of surfaces of mirrors exposed during the second campaign of JET-ILW in the base and in the outer divertor: (a) survey image with dust particles and peeled-off deposits; (b) spherical Fe+Ni droplet; (c) spherical Ni droplet; (d) spherical tungsten ball-like particle.
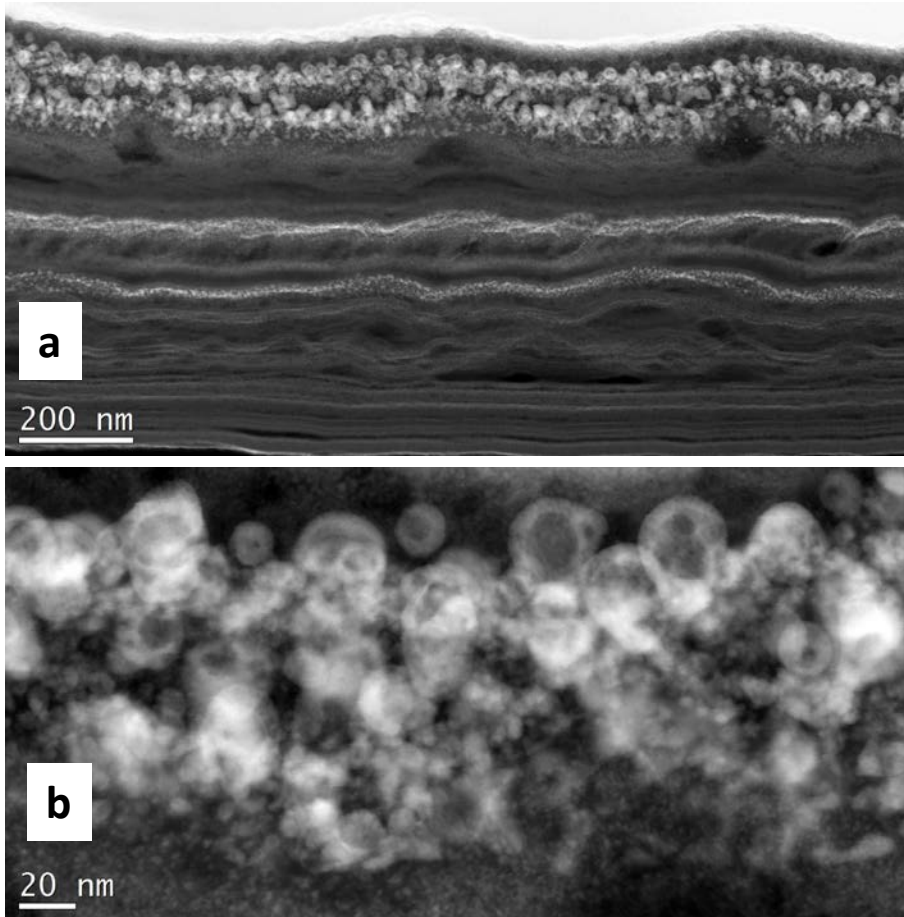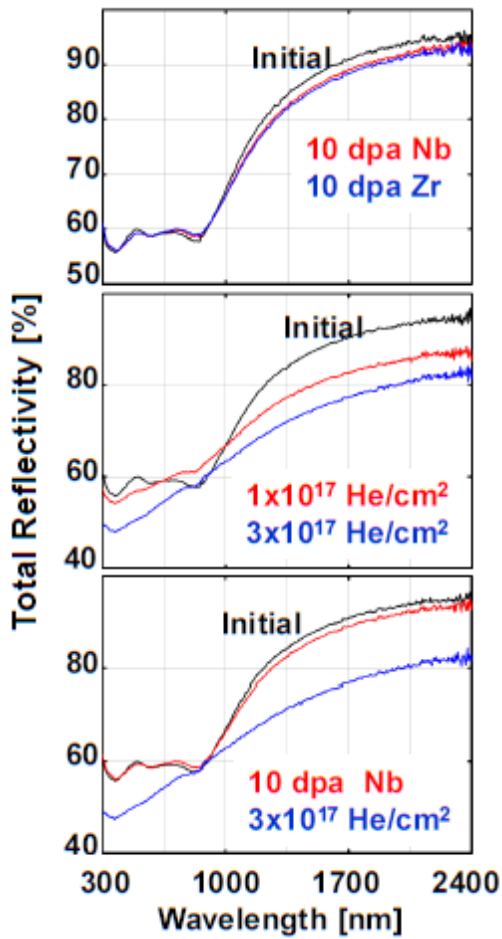
Figure 5

Figure 6

Transmission electron microscopy of the co-deposit from the inner divertor mirror: (a) overview image and (b) details of the structure.
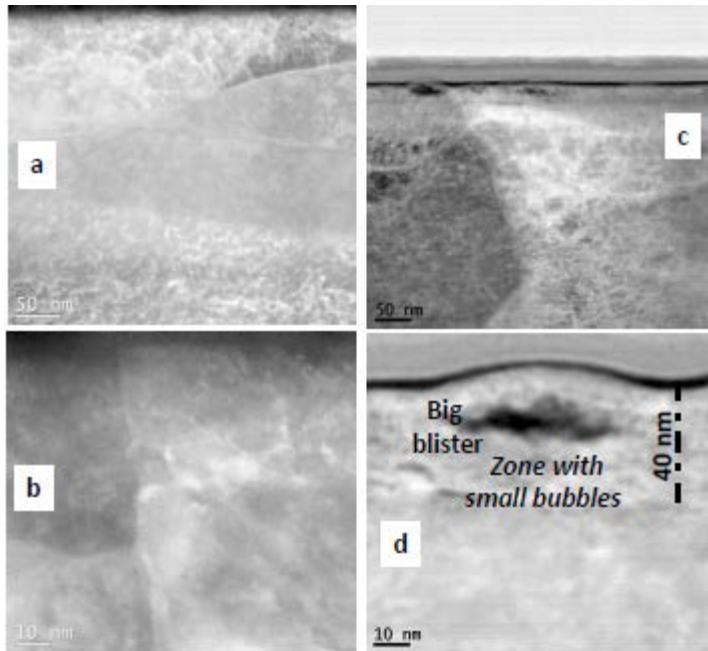
Figure 7

Variation of reflectivity of molybdenum mirrors under: (a) irradiation with $^{90}Nb^+$ corresponding to 10 dpa; (b) He^+ irradiation with two different fluency levels; (c) Irradiation with $^{90}Nb^+$ and $^4He^+$ ions.

Figure 8

Results of scanning transmission electron microscopy of molybdenum mirrors irradiated with: (a) and (b) with $^{90}Nb^+$ ions; (c) and (d) both with $^{90}Nb^+$ and with $^4He^+$ ions.

Figure 9.

Micrographs of the (a) surface and (b) sub-surface region of the Mo mirror irradiated first with ^{90}Nb$^+$ and then with helium and hydrogen ions.